PAX6 Suppresses the Invasiveness of Glioblastoma Cells and the Expression of the Matrix Metalloproteinase-2 Gene

Debra A. Mayes,[1] Yuanjie Hu,[1] Yue Teng,[1] Eric Siegel,[2] Xiaosong Wu,[1] Kishori Panda,[1] Fang Tan,[4] W.K. Alfred Yung,[4] and Yi-Hong Zhou[1,3]

Departments of [1]Neurobiology and Developmental Sciences and [2]Biostatistics, and [3]Arkansas Cancer Research Center, University of Arkansas for Medical Sciences, Little Rock, Arkansas and [4]Departments of Neuro-Oncology, The University of Texas M.D. Anderson Cancer Center, Houston, Texas

Abstract

Glioblastoma multiforme (GBM) is the most invasive brain tumor. We have previously reported that the transcription factor PAX6 suppresses the tumorigenecity of GBM cells. By an *in vitro* Matrigel invasion assay on two GBM cell lines stably transfected with wild-type and/or two mutant forms of PAX6, this study displays the first evidence that PAX6 inhibits the invasiveness of GBM cells and that the DNA-binding domain of PAX6 is required for this function. Using real-time quantitative reverse transcription-PCR (RT-PCR), gelatin zymography, and immunohistochemistry assays, the expression of the gene encoding matrix metalloproteinase-2 (MMP2) in GBM cell lines grown *in vitro* or in intracranial xenografts in nude mice was shown to be repressed by either stable or adenoviral-mediated overexpression of PAX6. Luciferase promoter assays revealed PAX6-mediated suppression of *MMP2* promoter activity. Electrophoretic mobility shift assays showed direct binding of PAX6 to the *MMP2* promoter. A significant reverse correlation ($P < 0.05$) occurred between *PAX6* and *MMP2* expression quantified by real-time quantitative RT-PCR in 41 GBMs, 43 anaplastic astrocytomas, and 7 adjacent normal tissues. Interestingly, the degree and significance of the reverse correlation increased after excluding astrocytomas, whereas it became insignificant after excluding GBMs. In GBM cells stably transfected with a dominant negative mutant PAX6 showing increased *MMP2* expression and invasiveness, knockdown of MMP2 revealed that *MMP2* is one of the PAX6 target genes mediating its suppression of invasion. Overall data delineated a mechanism for the suppressive function of PAX6 in GBM: suppression of cell invasion by repressing the expression of proinvasive genes such as *MMP2*. (Cancer Res 2006; 66(20): 9809-17)

Introduction

Glioblastoma multiforme (GBM) is the highest grade (WHO grade 4) of glioma with astrocytic cell features, which accounts for >60% of all primary malignant brain tumors. Patients diagnosed with GBM have an average survival time of 9 to 12 months, and <3% are living 5 years after diagnosis (1). A majority of GBM develop *de novo* (primary) whereas a small portion of GBM develop progressively from lower-grade astrocytomas (secondary) over a clinical course of generally 5 to 10 years (2). Primary and secondary GBMs are indistinguishable based on the following histologic hallmarks: microvascular hyperplasia, high infiltration of microglia, and central necrosis surrounded by a pseudopalisading layer, which distinguish from the lower-grade (WHO grade 3) anaplastic astrocytoma. In addition, GBM cells are highly invasive, making complete operational removal of the tumor impossible. Despite advances in surgery and radiotherapy, the outcome for patients with GBM has not significantly improved. Chemotherapy has only contributed marginal patient benefit (3–5).

Our recent studies have shown that the transcription factor *PAX6* has a tumor suppressor function in GBM cells (6). *PAX6* expression is significantly reduced in GBM compared with adjacent normal tissue or astrocytoma, and high expression is associated with a favorable outcome (7). *PAX6* is an evolutionarily highly conserved gene of the PAX family encoding transcription factors characterized with a paired DNA binding domain. PAX6 has conserved functions in the development of the eye and central nervous system (8, 9). Unlike most other developmental genes, its expression is sustained into adulthood in certain areas of the brain, including certain septal, diencephalic, and midbrain nuclei (10), and in astrocytes and certain mature neurons of the dentate gyrus (11). Using homozygous and chimera PAX6 mutant mouse/rat models, the function of PAX6 in cell migration during development has been well studied. In those studies, PAX6 was shown to act as a migration control gene during development, critical for correct migration of cells into several areas including the eye (12), olfactory bulb (13), cortex (14, 15), and cerebellum (16). Exactly how PAX6 controls cell migration in these areas during development is not clear.

GBM is characterized by extensive brain invasion, which may be mediated by proteinase modulation of the extracellular matrix. Studies focusing on the mechanisms of GBM invasion suggest that matrix metalloproteinases (MMP) play critical roles in this process (17–19). In addition to enhancing tumor cell invasion by degrading extracellular matrix proteins (20), MMPs stimulate tumor progression by solubilizing extracellular matrix-bound growth factors (21, 22) and cleaving and activating other growth factors, such as transforming growth factor β (21), which are implicated in GBM motility, angiogenesis, and proliferation (23, 24). In fact, both MMP2 mRNA and protein levels are elevated in malignant gliomas (25–30). Local invasiveness is the primary cause of GBM treatment failure; therefore, understanding the mechanisms involved in tumor invasion within the brain is vital to controlling this disease. We report here that PAX6 can suppress both GBM cell invasion and the expression of *MMP2 in vitro* and *in vivo*. These observations may provide insights into the molecular mechanisms underlying GBM progression as well as providing implications about the role of PAX6 in cell migration during embryonic development.

Requests for reprints: Yi-Hong Zhou, University of California, Irvine, 101 The City Drive, Building 56, Suit 400, Zot 5397, Orange, CA 92868. Phone: 949-824-5767; Fax: 714-456-8284; E-mail: yihongz@uci.edu.

doi:10.1158/0008-5472.CAN-05-3877

Materials and Methods

GBM cell lines and stable transfectants. The human GBM cell lines U251HF, U87, and LN229 were obtained from the Department of Neuro-Oncology, The University of Texas M.D. Anderson Cancer Center. Our U87 and LN229 cells have the same mutation in the *TP53* gene as described by Ishii et. al. (31). U251HF, also named HF U-251, has the same homozygous mutation in the *TP53* gene as occurs in the commonly used U251MG cell line: CGT (Arg) to CAT (His) at codon 273. However, U251HF has a lower level of *PAX6* expression than that found in U251MG, and, according to Ke et al. (32), has high tumorigenecity—comparable to that of U87. In contrast, the tumorigenecity of U251MG is low. All cell lines and stable transfectants were cultured in DMEM/F12 medium supplemented with 5% calf serum and 1× penicillin-streptomycin (Invitrogen, Carlsbad, CA).

PAX6 stable transfectants of U251HF were generated in a previous study (6). The same method was used to stably transfect two mutant forms of PAX6, dmt and 344 (see Fig. 1*B*), and generate PAX6 stable transfectants of LN229 (Fig. 1*E*). The PAX6-344 expression construct has previously been described (6). We generated the dmt construct by introducing two missense mutations (R26G and I87R) in the paired domain using PCR-based point-direct mutagenesis (33).

Stable knock-down of MMP2 in 344-transfected cells by retroviral transduction of shMMP2 construct. The retroviral construct MMP2-shRNA/pSM2 (V2HS-48431) was obtained from Open Biosystems (Huntsville, AL). The shMMP2 retrovirus was produced by cotransfection of 239 cells stably transfected with pVPack-VSV-G (gift from Dr. T.J. Liu, Department of Neuro-Oncology, The University of Texas M.D. Anderson Cancer Center, Houston, TX) with the MMP2-shRNA/pSM2 and pVPack-GP (Stratagene, La Jolla, CA) using FuGENE6 (Roche, Indianapolis, IN) and grown for 2 days. Then an aliquot of the medium containing the secreted retrovirus was added to attached subconfluent U251HF(344-1) cells, and stably transfected clones were selected by puromycin.

Adenoviral infection. Replication deficient adenovirus expressing PAX6 (Ad-PAX6) and 344 (Ad-344) was described in our previous study (6). Adenovirus expressing green florescent protein (Ad-GFP) was a gift from Dr. T.J. Liu. Glioma cells (400,000 per 35-mm well) were plated in culture medium overnight, then washed twice with PBS, and infected with adenovirus at a concentration of 50 viral particles per cell in 0.5 mL of serum-free medium. One hour later, 1.5 mL of serum-free medium were added to the cells, and they were allowed to grow for 48 hours before condition medium was harvested and RNA extracted.

RNA, cDNA, and LightCycler real-time quantitative reverse transcription-PCR of cells, xenografts, and gliomas. RNA from intracranial xenografts of U251HF or its two PAX6 stable transfectants (PAX6-2.2, and PAX6-2.3; ref. 6) and RNA from cells grown *in vitro* were extracted using Trizol and converted to cDNA using SuperScript RT II (Invitrogen).

Quantification of the expression of human genes [*β-actin, enolase-α*, glyceraldehyde-3-phosphate dehydrogenase (*GAPDH*), *MMP2*, and *PAX6*] in gliomas (41 GBMs and 43 astrocytomas) and seven adjacent normal tissues were described in our previous study (7, 30). Primers in real-time quantitative reverse transcription-PCR (RT-PCR) shown below amplify only human genes, not the mouse homologue, as determined using the cDNA from control mouse brain (data not shown) for *β-actin*, 5′-TCCTTCC-TGGGCATGGAGT-3′ and 5′-GCCATGCCAATCTCATCTTG-3′; *GAPDH*, 5′-CAGGAGGCATTGCTGATG-3′ and 5′-CAATATGATTCCACCCATG-3′; *enolase-α*, 5′-AGTGGCTAGAAGTTCACC-3′ and 5′-TGGCAGGATGACTTC-AGA-3′; and *MMP2*, 5′-ATGGATCCTGGCTTTCCC-3′ and 5′-GCTTCCAAAC-TTCACGCTC-3′. The same gene-specific standards included in the assay for quantitative results were used as in our previous studies (7, 30) except for *GAPDH*. A new standard for the above GAPDH primers were made with the primer set 5′-AGCCGAGCCACATCGCTCA-3′ and 5′-TGCAGGAGGCA-TTGCTGATG-3′. Real-time quantitative RT-PCR was conducted as previously reported (30). The real-time quantitative RT-PCR for each cDNA sample was repeated at least twice and the mean value was taken for statistical analysis.

Western blot and immunohistochemistry assays. Whole-cell lysate extraction and Western blotting were previously described (17). Antibodies against PAX6 (1:1,500 dilution) was described previously (34) and actin (1:5,000 dilution) from EMD Bioscience (San Diego, CA). For immunohistochemistry, paraffin sections of intracranial xenografts were deparaffinzed and treated with Citra Antigen Retrival Solution following a microwave pressure cooker procedure (BioGenex, San Ramon, CA). Rabbit anti-MMP2 antibody (Chemicon, Temecula, CA) at 1:500 dilution was incubated at 4°C overnight. Secondary antibody (biotin-goat anti-rabbit from BioGenex) and labeling steps were done at room temperature for 30 minutes each. A DAB kit (BioGenex) was then used to stain the reactions. The nucleus was counterstained with Harris hematoxylin.

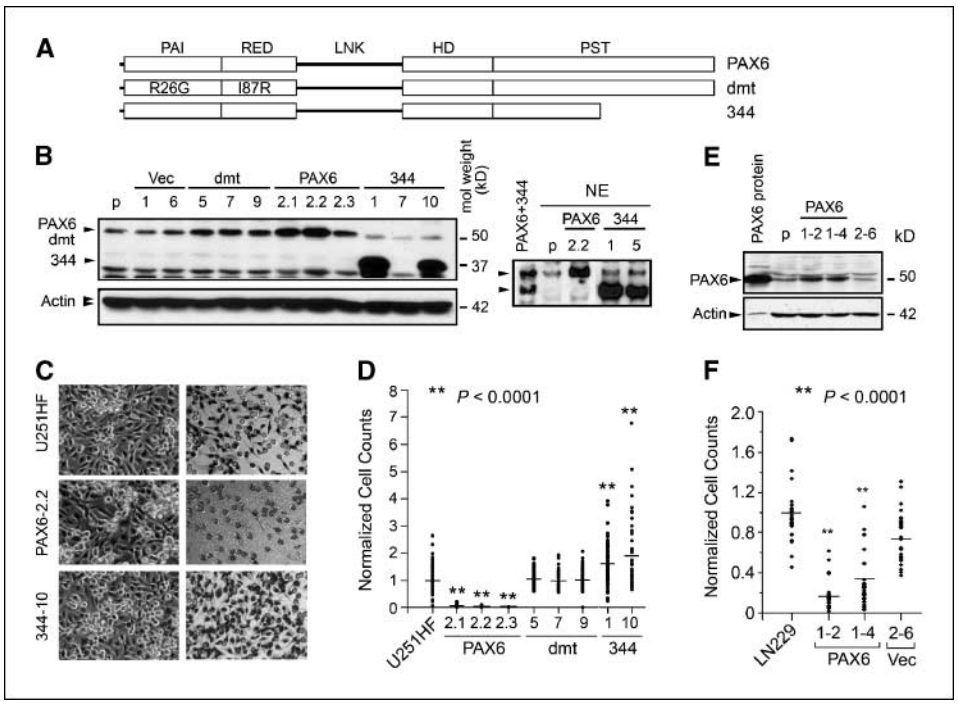

Figure 1. Stable overexpression of *PAX6* in GBM cells suppresses cell invasiveness. *A,* depiction of PAX6 mutation constructs. Western blotting using polyclonal PAX6 antibody in whole-cell lysate or nuclear extract of U251HF (*B*) and whole-cell lysate of LN229 (*E*) determined positive stable transfectants of wild-type and mutants of PAX6. *p,* parental wild-type GBM cell line; *Vec,* vector transfectants. PAX6 and 344 *in vitro* synthesized proteins were made from plasmid constructs in pRC-CMV vector using TnT T7 Quick Transcription/Translation System (Promega, Madison, WI) and used as a control for PAX6 antibody. Actin antibody detected actin in the same blot after stripping as control of protein loading. *C,* representative pictures of cells above Matrigel (*left*) and cells that invaded through Matrigel (*right*) after 16 hours of culture. *D* and *F,* comparison of cell invasiveness of GBM cell lines U251HF and LN229, respectively, after stable transfection with wild-type or mutant PAX6. The position of the bar is the mean of the normalized cell counts from duplicate or triplicate invasion assays of three to five independent experiments. Bonferroni-adjusted $P < 0.0001$ from Wilcoxon rank-sum tests was used for statistically significant difference between groups.

Gelatin zymography. Equal numbers of GBM cells/transfectants were plated in DMEM/F12 containing 5% calf serum overnight to reach 80% confluency. The conditioned medium was collected after removal of floating cells. Proteins in the medium were precipitated with 4 volumes of cold acetone, spun immediately at 14,000 rpm for 5 minutes at 4°C, and resuspended in radioimmunoprecipitation assay buffer containing 1× Protease Inhibitor Cocktail (Roche). Gelatin zymography was done using equal amounts of protein (0.1-0.3 μg for LN229, 0.5-1 μg for U87, and 2-4 μg for U251HF) as previously described (35). Protein readings were based on the control for correct protein loading, and each experimental sample was repeated two to three times to verify the results.

Tumor cell Matrigel invasion assay. Matrigel Basement Membrane Matrix (Becton Dickinson Labware, Badford, MA) was used for *in vitro* cell invasion assays. U251HF or LN229 GBM cell lines and their PAX6 stable transfectants were seeded (5×10^5-7.5×10^5 in 0.7 mL DMEM/F12) in duplicate or triplicate onto Costar Transwells (12-mm diameter, 12-μm pore size) coated with 200 μL Matrigel (1 mg/mL). DMEM/F12 medium (1 mL) supplemented with (for U251HF) or without (for LN229) calf serum (0.05%) was added to the outside of the transwell. After 16 hours, cells that had invaded through the Matrigel and migrated to the lower surface of the filter were stained with a HEMA3 staining kit (Fisher Scientific, Houston, TX) and counted. Pictures of randomly picked microscope fields at ×200 magnification were taken (10 fields per filter) and cells were counted. The number of transfected cells that migrated through the Matrigel was normalized by the mean cell count for the parental cells in each invasion experiment. Data from three to four independent experiments were combined, plotted, and subjected to statistical analysis.

Human *MMP2* promoter-luciferase constructs and luciferase assays. We used a nested PCR strategy to amplify a 2,376-bp MMP2 DNA fragment (MMP2P1) including the promoter (1,780 bp upstream of the major transcriptional initiation site ref. 36) and the 5′-untranslated region (5′-UTR; 433-bp exon 1 and 139-bp 5′ intron 1) from the DNA of normal human blood cells. This DNA fragment was then cloned into the pGL3B luciferase reporter vector (Promega, Madison, WI) via *Sac*I and *Xho*I, and the sequence was verified by sequencing. Shortened *MMP2* promoter constructs, such as MMP2P5/pGL3B and MMP2P6/pGL3B, were made based on MMP2P1/pGL3B via restriction enzyme digestions.

Cells (250,000 per 35-mm well) were plated overnight, and the culture medium was changed to serum-free medium before transfection with 1 μg *MMP2* gene promoter luciferase constructs (MMP2P1, MMP2P5, or MMP2P6) using 3 μL of FuGENE6 transfection reagent per well (Roche). Cells were cotransfected with 0.1 μg of pRL-CMV expressing Renilla luciferase as an internal control. Forty-eight hours after transfection, cell lysates were extracted and luciferase activity was measured using a Dual-Luciferase Reporter Assay System (Promega) and a TD-20/20 Luminometer (Turner Designs, Sunnyvale, CA).

Electrophoretic mobility shift assay. MMP2P5-1 DNA fragment was amplified by PCR with a primer set (5′-CGGCCGGGGAAAAGAGGTG-3′ and 5′-AATCCCTTTGTATGTTTAAAGC-3′) from the MMP2P5/pGL3B construct and cloned into pCR4.0 (Invitrogen). After sequence verification, the MMP2P5-1 DNA fragment was cut out by *Eco*RI digestion and gel purified using QIAquick columns (Qiagen, Valencia, CA). MMP2P5-1 DNA was labeled with [α-^{32}P]dATP (3,000 Ci/mmol) using Klenow polymerase as previously described and used in each binding reaction with *in vitro* synthesized PAX6 protein using TnT T7 Quick Transcription/Translation System (Promega) with each cDNA cloned in pRC-CMV vector or nuclear extract as previously described (37).

Statistical analysis. Mixed model ANOVAs with standard post hoc comparison methods were used to test for differences in MMP2 RNA, protein levels, and promoter activity between multiple stable transfectants and the parental cell line U251HF, and for differences in MMP2 RNA and protein levels between adenovirus-infected cells and mock infection. Wilcoxon rank-sum tests with normal approximation were used to compare each difference on normalized cell counts in Matrigel invasion assays, with two-sided Bonferroni-adjusted *P* values being reported. Spearman rank correlation tests were used to examine possible paired correlations among the gene expressions in malignant astrocytomas. All statistics were conducted by SAS 9.1 software (SAS Institute, Inc., Cary, NC).

Results

PAX6 suppresses the *in vitro* invasion ability of GBM cells. To characterize the role of PAX6 in GBM, we established PAX6 stable transfectants in two GBM cell lines with high tumorigenecity, U251HF and LN229. We also established stable transfectants in U251HF with two PAX6 mutants, 344 and dmt. PAX6-344 has a truncation mutation in the PST domain leaving only 75 functional PST codons of the 153 total codons. This mutation has also been shown to predispose patients to aniridia (38) and has been shown to have a dominant negative function via competitive binding with wild-type PAX6 at its target sequences (39). PAX6-dmt contains two missense mutations (R26G and I87R) in two subdomains of paired domain, each of which has been identified in aniridia patients and has been shown to abolish the binding activity of PAX6 (34, 37). Western blotting with PAX6 antibody confirmed positive transfectants of PAX6 (PAX6-2.1, PAX6-2.2, and PAX6-2.3), PAX6-344 (1, 5, 9, and 10), and PAX6-dmt (5, 7, and 9) in U251HF and LN229 (1-2 and 1-4), and representative Western blots were shown in Fig. 1*B* and *E*. Western blots using a FLAG antibody to detect the expression of exogenous PAX6 and 344 have previously been shown (6). Western blots using nuclear extracts indicated that PAX6-344 retained its ability to enter the nucleus (Fig. 1*B, right*).

Because GBM is highly invasive, we investigated the function of PAX6 on invasion using Matrigel invasion assays. As shown in Fig. 1*C* (*left*), there is no marked change in the ability of the cells to attach to Matrigel in either the parental or the stable transfected cells after being seeded in serum-free medium. When the same concentration of cells and the same culture conditions were applied in Matrigel invasion assay, as shown in Fig. 1*C* (*right*) and *D*, the invasiveness of U251HF cells was significantly reduced (almost abolished) after stable transfection with PAX6 ($P < 0.0001$ for all three positive PAX6 transfectants examined). In contrast, the invasion ability of U251HF cells was significantly enhanced after stable transfection with PAX6-344 ($P < 0.0001$ for the two positive PAX6-344 transfectants examined) but not significantly affected after stable transfection with PAX6-dmt.

Similar suppression by PAX6 on cell invasiveness was also observed in another GBM cell line, LN229 (Fig. 1*F*), in which two positive PAX6 transfectants were examined. Thus, PAX6 is directly involved in suppressing *in vitro* cell invasion within two GBM cell lines. Importantly, our data suggest that the DNA-binding function of PAX6 is critical for such suppression, suggesting that the gene(s) responsive for glioma cell invasion may be directly regulated by PAX6. Data shown below show that *MMP2* is one of these genes.

Stable transfection-mediated overexpression of PAX6 suppresses *MMP2* expression in GBM cells *in vitro* and in intracranial xenografts. To study the function of the tumor suppressive activities of PAX6 observed in U251HF (6), we did RNA hybridization against the Human Genome U133A oligo chips (Affymetrix, Santa Clara, CA). These studies revealed a decrease in *MMP2* expression by PAX6 when we compared the gene expressions of two *in vitro* cultured PAX6 stable transfectants (PAX6-2.2 and PAX6-2.3) and two control cells (the parental and vector transfectant v1). Similar results were found when we compared the gene expressions of U251HF subcutaneous xenografts (combination of five tumors) and PAX6-2.2 subcutaneous xenografts (combination of seven tumors), removed 20 days after implantation (data not shown).

MMP2 expression was then quantified in cells from *in vitro* cultures by real-time quantitative RT-PCR and normalized to either *GAPDH* or *enolase-α*. In agreement with data from above-described microarray, the results showed that, compared with control cells (parental and vector transfectants) after normalizing to either *GAPDH* or *enolase-α* (Fig. 2*A*), *MMP2* expression was significantly lower in PAX6 transfectants, with averages of 42% and 44% of control after normalizing to *GAPDH* and *enolase-α*, respectively ($P < 0.001$ for both). In agreement with our data on cell invasiveness shown in Fig. 1*D*, *MMP2* expression was significantly higher in 344 transfectants, with averages of 148% and 240% of control after normalizing to *GAPDH* ($P < 0.05$) and *enolase-α* ($P < 0.001$), respectively, but not significantly altered in dmt transfectants ($P > 0.05$). Gelatin zymography assays showed a single clear band at ~72 kDa, indicating MMP2-mediated gelatin degradation, and these studies confirmed similar changes at the protein level (Fig. 2*B* and *C*).

Based on our unpublished data from real-time quantitative RT-PCR and zymography, the MMP2 level in LN229 is ~10-fold higher than that in U251HF. PAX6 stable expression in LN229 showed a decrease of *MMP2* expression to 60% to 70% of the level of the parental or vector-transfected LN229 cells (data not shown). Overall, our data indicate that PAX6 suppresses *MMP2* expression in GBM cells grown *in vitro*.

To determine whether PAX6-mediated suppression of *MMP2* expression in GBM cells grown *in vitro* remains in a brain *in vivo* environment, we examined the *MMP2* expression in intracranial xenografts derived from three U251HF xenografts and four PAX6 transfectant xenografts (two for PAX6-2.2 and two for PAX6-2.3). The survival of these nude mice has been reported in our previous study (6). As shown in Fig. 3*A* (*a* and *b*), immunohistochemistry displayed uniform cytoplasmic staining for MMP2 in U251HF intracranial xenografts, especially in cells surrounding the tumor, in infiltrating tumor cells, and in infiltrated tumor mass. The blue staining of nucleus pleomorphism with hematoxylin showed that the cells with positive MMP2 staining were tumor cells. Our data showed that stable overexpression of PAX6 suppresses the expression of *MMP2* in the tumor cells propagated *in vivo*; however, based on the data from this experimental model, it is not conclusive whether or not it also decreases the invasiveness *in vivo*.

We have observed that in the *in vitro* culture condition, PAX6 suppressed *MMP2* expression in U251HF cells by ~40%. In contrast, in the *in vivo* condition, a dramatic decrease of MMP2 staining in the intracranial xenografts of PAX6-transfected cells occurred compared with that derived from the wild-type U251HF (Fig. 3*A, c* and *d*). To confirm this observation, real-time quantitative RT-PCR was done on cDNA from these intracranial xenografts using a set of primers that specifically amplify human *MMP2* and internal control gene transcripts. As shown in Fig. 3*B*, after normalizing independently to three internal control genes (*enolase-α, β-actin*, and *GAPDH*), all six intracranial xenografts of PAX6 transfectants displayed a dramatic decrease (average 10% level of control) in *MMP2* expression when compared with the two intracranial xenografts from U251HF (control). Although one U251HF intracranial xenograft had similar levels of *MMP2* expression compared with that of most PAX6 transfectants, the survival time for that mouse (41 days) is close to the average survival time for the mice implanted with the PAX6 transfectants (43 days), reflecting experimental variation among animals. Combining data on *MMP2* expression in intracranial xenografts at both the cellular and tumor mass levels as detected by immunohistochemistry and real-time quantitative RT-PCR,

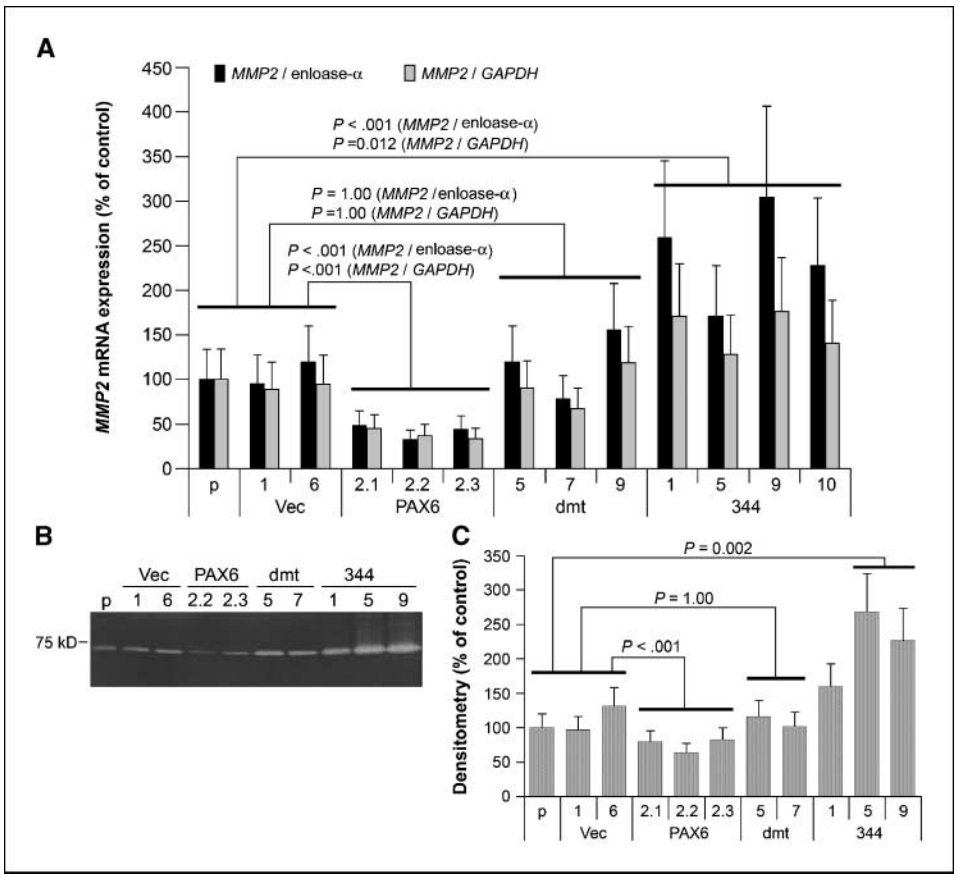

Figure 2. Stable overexpression of *PAX6* suppresses the expression of *MMP2* in U251HF cells grown *in vitro*. Attached subconfluent cells were cultured in serum-free medium for 48 hours before RNA extraction from attached cells and precipitation of secreted proteins, as described in Materials and Methods. *A,* real-time quantitative RT-PCR quantified *MMP2* expression ratios relative to *enolase-α* and *GAPDH*, expressed as percent of parental cells (*p*). *B,* a representative gelatin zymography gel. *C,* densitometry of gelatin degradation by MMP2. Data for statistical analysis were from three to six independent experiments. Expression ratios were log transformed to stabilize variance for mixed model ANOVA with Construct as fixed effect and Experiment as random effect. *Columns,* mean as calculated by back-transformation from the least-square means and ANOVA; *bars,* SD analyzed by mixed model ANOVA. Horizontal lines above the columns indicate Construct Groupings, with Bonferroni-adjusted *P* values shown for the indicated contrasts among Construct Groupings.

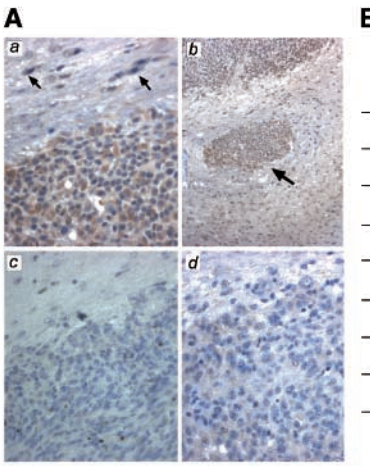

B

#	Cell	Survival Day	1000 X *MMP2* / control gene		
			Enolase-α	β-actin	GAPDH
1	U251HF	28	580	119	420
2	U251HF	28	201	195	158
3	U251HF	41	18	16	22
4	PAX6-2.2	38	2	4	4
5	PAX6-2.2	42	14	26	27
6	PAX6-2.2	51	7	25	60
7	PAX6-2.3	38	23	29	27
8	PAX6-2.3	45	9	26	50
9	PAX6-2.3	45	7	23	23

Figure 3. Stable overexpression of *PAX6* suppresses the expression of *MMP2* grown *in vivo*. *A,* representative MMP2 immunoreactivity in intracranial xenografts of U251HF (*a*, ×400; *b*, ×100), PAX6-2.3 (*c*, ×400), and PAX6-2.2 (*d*, ×400). *Small and large arrows,* infiltrating cells and infiltrated tumor with positive MMP2 staining, respectively. Positive MMP2 staining (*brown*) was shown in the cytoplasm of tumor cells whereas the nucleus was stained blue with hematoxylin. *B, MMP2* expression ratios times 1,000 relative to *enolase-α, β-actin*, or *GAPDH* in intracranial xenografts of U251HF, PAX6-2.2, and PAX6-2.3, each quantified in real-time quantitative RT-PCR by the human gene-specific primers and the gene-specific standards. For survival days of the animal, refer to Zhou et al. (6).

respectively, the data indicate that *MMP2* expression in the GBM cell line U251HF was markedly reduced by stable expression of PAX6 in a physiologically relevant *in vivo* setting.

Adenoviral-mediated overexpression of *PAX6* suppresses *MMP2* expression in multiple GBM cell lines. To determine if PAX6-mediated suppression of *MMP2* expression generally occurs in different GBM cell lines and if transient overexpression of PAX6 has the same suppression effect on *MMP2* expression as it does after stable overexpression, three high tumorigenic GBM cell lines (U251HF, U87, and LN229) were infected with replication-deficient recombinant adenovirus expressing PAX6 (Ad-PAX6), 344, the truncation mutant of PAX6 (Ad-344), or green fluorescent protein (Ad-GFP). All three cell lines express low levels of PAX6 (7), however, they differ in their *p53* and phosphatase and tensin homologue (*PTEN*) mutation status. U251HF and LN229 have homozygous *p53* mutations on R273H and P98L, respectively (6),[5] whereas U87 cells are wild-type for *p53* (31).

Western blot analysis confirmed the overexpression of PAX6 and PAX6-344 protein in these cells (data not shown) before quantitative RT-PCR and gelatin zymography assays were done. After normalizing to *GAPDH* or *enolase-α*, results from real-time quantitative RT-PCR showed a significant reduction of *MMP2* expression in the Ad-PAX6–infected cells when compared with the mock-infected cells for all three GBM cell lines (Fig. 4*A-C*). In contrast to the results after stable overexpression of 344 in U251HF, cells displayed no significant differences in *MMP2* expression after the infection of Ad-344. As expected, cells displayed no significant differences in *MMP2* expression after being infected with Ad-GFP. Data from gelatin zymography assays (Fig. 4*D*) support the data from real-time quantitative RT-PCR in U251HF cells.

Interestingly, *MMP2* expression in LN229 cells was also suppressed by Ad-344, although to a lesser extent than with Ad-PAX6. However, the secreted MMP2 level was not altered 48 hours after infection (Fig. 4*E*). In U87 cells, *MMP2* expression was suppressed by either Ad-PAX6 or Ad-344, but the secreted MMP2 level was not found to be significantly altered 48 hours after infection (Fig. 4*F*). Overall data revealed a consistent transient suppression of *MMP2* transcription by PAX6 in all three GBM cell lines and differential effects on secreted MMP2 levels from these cells.

PAX6 suppresses *MMP2* expression by decreasing *MMP2* promoter activity. PAX6 is a transcription factor. Data from the above study showed that wild-type PAX6 expression down-regulates the level of *MMP2* RNA, up-regulates *MMP2* after the expression of the PAX6 COOH-terminal truncation mutant, which contains intact DNA binding domains, and has no effect after the expression of the PAX6 mutant lacking DNA binding capability, suggesting that PAX6-mediated suppression of *MMP2* expression may occur via direct binding to the *MMP2* promoter. Luciferase assays were carried out to estimate the activity of the *MMP2* promoter in U251HF and its stable transfectants of PAX6, dmt and 344. As illustrated in Fig. 5*A*, we inserted two fragments of the *MMP2* promoter (MMP2P1 and MMP2P5, 1,780 and 177 bp upstream of the major transcription initiation site, respectively; ref. 36) upstream of a luciferase reporter in the pGL3B vector. Because it is common for *cis*-elements in the 5′-UTR to be involved in transcriptional regulation, we included exon 1 and part of intron 1 into these two luciferase constructs.

As shown by the *black column* in Fig. 5*B*, luciferase activity of MMP2P1/pGL3B was significantly lower in the PAX6 stable transfectants (PAX6-2.2 and PAX6-2.3) when compared with the wild-type cells ($P < 0.01$). Similar results were obtained when using the MMP2P5/pGL3B construct (including a 177-bp region upstream of the transcription initiation site and a 596-bp 5′-UTR), narrowing the PAX6 responsive region to 773 bp (Fig. 5*B, white column*).

To further narrow the responsive region, we made a shorter *MMP2* promoter construct, MMP2P6, which contains the 177-bp promoter and 248-bp 5′ region of exon 1 (Fig. 5*A*). As shown by the gray column in Fig. 5*B*, the luciferase activity of MMP2P6/pGL3B remains to be significant lower in the PAX6-transfected cells compared with control (untransfected parental cells). In contrast, it was significantly higher in the 344-transfected cells but not significantly changed in dmt-transfected cells. Overall data showed changes in *MMP2* promoter activities in response to the stable expression of exogenous wild-type PAX6. The effects of both the PAX6 dominant negative and null mutants on DNA binding are in accordance with the changes seen in endogenous *MMP2* expression and cell invasiveness.

The data shown are not limited to the U251HF cell line. In LN229 cells stably transfected with PAX6, *MMP2* promoter activities shown by MMP2P5/pGL3B and MMP2P6/pGL3B were also significantly lower compared with the untransfected parental

[5] S. Griffin, unpublished data.

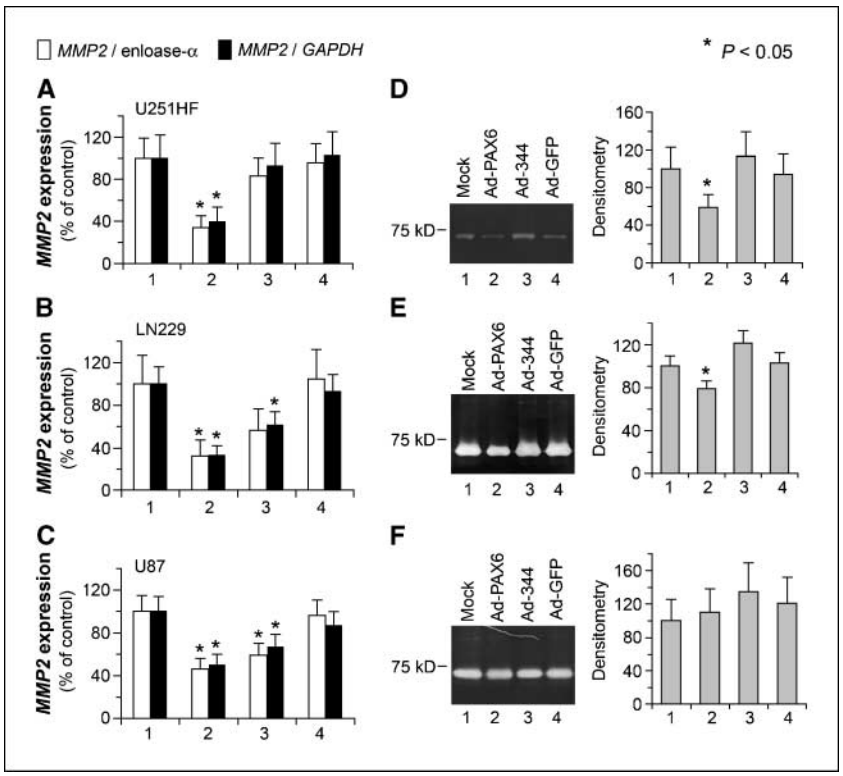

Figure 4. Adenoviral-mediated overexpression of *PAX6* suppresses *MMP2* expression in malignant GBM cell lines U251HF, LN229, and U87 *in vitro*. Equal amounts of cells were infected with Ad-PAX6 (*lane 2*), Ad-344 (*lane 3*), and Ad-GFP (*lane 4*; 50 viral particles per cell) and incubated in serum-free medium for 48 hours before extraction of RNA and precipitation of secreted protein. Mock infection (*lane 1*) was used as a control. *A* to *C,* comparison of *MMP2* expression quantified by real-time quantitative RT-PCR and normalized to *GAPDH* (*black column*) or *enolase-α* (*white column*). *D* to *F,* representative gelatin zymography of U251HF (4 μg protein per lane), LN229 (0.6 μg protein per lane), and U87 (1.5 μg protein per lane), respectively. *Right,* densitometry of the MMP2 band. *Columns,* group mean from three to five independent experiments as calculated by back-transformation from the least-square means and ANOVA; *bars,* SD analyzed by mixed model ANOVA. Post hoc comparisons were of infection (noncontrol) to mock (control) of each cell line. Symbols above noncontrol columns indicate Bonferroni-adjusted *P* values for difference from control.

cells (Fig. 5*C*). Overall data show that PAX6 suppresses *MMP2* promoter activity via *cis*-elements located within a 425-bp region surrounding the transcription initiation site in two GBM cell lines.

PAX6 binds directly to the *MMP2* promoter *in vitro* and *in vivo*. The promoter assay data shown above suggested that PAX6 regulation of *MMP2* expression may occur via direct binding of PAX6 DNA-binding domains to the MMP2 promoter. Electrophoretic mobility shift assay (EMSA) was done using either *in vitro* synthesized proteins (PAX6, PAX6-344, or PAX6-dmt) or nuclear extract from U251HF cells with a PCR-amplified DNA fragment corresponding to the 5′ portion of MMP2P6, MMP2P5-1 (−177 to +68; displayed in Fig. 5*A*). The 3′ portion of MMP2P6 (+68 to +248) is highly G/C rich (81%) whereas previously identified PAX6 binding sites are not G/C rich (37, 40); therefore, we did not examine this region for PAX6 binding.

As shown in Fig. 5*D* (*lanes 2* and *3*), both PAX6 and PAX6-344 were able to bind to MMP2P5-1. The binding specificity was estimated by addition of excessive amounts (5×-50×) of the unlabeled, PAX6-specific binding oligomer Tsp11Bs, its nonfunctional mutant oligomer Tsp11Bm1 (37), or paired domain-specific binding oligomer CD19-2(A) (40). Binding of PAX6 to MMP2P5-1 was competed out by increasing the amount of the unlabeled PAX6-specific binding probe Tsp11Bs (*lanes 4-6*), but not the mutant probe Tsp11Bm1, which is only 4 bp different from Tsp11Bs (*lanes 7-9*). This data indicates that PAX6 binds in a sequence-specific manner to MMP2P5-1. CD19-2(A) was also able to compete out PAX6 or PAX6-344 binding to MMP2P5-1 (*lane 10*). In addition, the PAX6 rabbit polyclonal antibody supershifted the PAX6/MMP2P5-1 complex (*lane 11*), whereas the rabbit polyclonal antibody C-Myb failed (*lane 12*).

It seems that there is a non-PAX6/MMP2P5-1 complex at a size similar to PAX6/MMP2P5-1 complex; therefore, to clearly show MMP2P5-1 binding to PAX6 DNA-binding domains, we examined MMP2P5-1 binding using serial competitors to the truncation mutant PAX6-344. As shown in Fig. 5*D*, the PAX6-344/MMP2P5-1 complex migrates faster than the PAX6/MMP2P5-1 complex and can be specifically competed by competitors for PAX6 (*lanes 14-16*) or paired domain 6 specific binding (*lane 20*), but not the mutant oligomer (*lanes 17-19*). Furthermore, the binding of 344 to MMP2P5-1 failed to be competed by control antibody (*lane 22*) but was abolished by PAX6 antibody (*lane 21*), which contrasts to the supershift noted with PAX6/MMP2P5-1. The antibody was added before the addition of the labeled probe; therefore, the deletion of the COOH-terminal portion of PAX6 may affect protein folding and binding of the PAX6 antibody could have blocked protein binding. The double mutant protein PAX6-dmt has point mutations in PAX6 DNA binding domains and failed to have sequence-specific binding as expected (data not shown).

Serial competition in EMSA by PAX6-specific binding oligomers, mutant oligomer, and PAX6 antibody, in addition to the supershifted protein complex shown after PAX6 antibody addition, provided solid data showing that both PAX6 and PAX6-344 bind in a sequence-specific manner to the MMP2P5-1 region in the *MMP2* promoter. EMSA done using nuclear extract from U251HF cell indicated that PAX6 also binds to MMP2P5-1 *in vivo* (Fig. 5*D*, *lane 23*), which can be competed by CD19-2(A) (Fig. 5*D*, *lane 24*). Overall, it is evident that there is a PAX6-specific binding site in a 245-bp region (−177 to +68) of the *MMP2* promoter. PAX6 binding to this region is sequence specific and requires the paired domain but not the COOH-terminal PST domain.

MMP2 is one of the PAX6 target genes mediating PAX6 suppression of glioma cell invasion. To determine how critical PAX6 suppression of *MMP2* expression in GBM cells is to the suppression of cell invasion, we knocked down the level of MMP2 in 344-1 cells (a line of 344-transfected U251HF) by transduction of

a shMMP2 retroviral construct (Fig. 6*A*). Matrigel invasion assays showed a significant decrease of cell invasiveness corresponding to the decrease of MMP2 levels in 344-1 cells (Fig. 6*B*), indicating that MMP2 is responsible for the increase in invasiveness after stable transfection with 344.

Interestingly, although the endogenous MMP2 level in 344-1(shMMP2)-9 cells was lower than that in PAX6 transfected cells, there was no significant difference on cell invasiveness compared with U251HF, in contrast to the almost abolished cell invasiveness by PAX6-2.2 cells. Therefore, the role of PAX6 in suppressing invasion is not limited to *MMP2*, and PAX6 may suppress other proinvasive genes. 344-1(shMMP2) cells, which had a higher degree of MMP2 knock-down (clones 1 and 5), showed significantly less invasiveness when compared with U251HF, suggesting that MMP2 does play a critical role in glioma invasion. Overall comparison of Matrigel invasiveness of wild-type, PAX6-transfected, and 344-transfected U251HF cells to 344-transfected cells with knock-down of MMP2 provided information indicating that MMP2 is one of the mediators of PAX6 affecting glioma cell invasiveness.

Reverse correlation between the expression of *PAX6* and *MMP2* in human GBMs but not in astrocytomas. MMP2 is known to be a proinvasive protease that is up-regulated in malignant gliomas. In our previous report using quantitative real-time PCR to compare *PAX6* and *MMP2* expression in malignant astrocytoma specimens with corresponding adjacent normal tissues, *PAX6* expression was 10% to 50% lower and *MMP2* expression was 10- to 60-fold higher in all GBMs compared with that in the corresponding adjacent normal tissues (30). Using data obtained in these previous two studies, we did Spearman rank correlation tests to compare *PAX6* and *MMP2* gene expressions in these malignant astrocytomas (41 GBMs and 43 anaplastic astrocytomas) and 7 adjacent normal tissues. The expression ratios relative to β-actin were plotted in Fig. 6*C*. The result showed a significant negative correlations ($R = -0.22$, $P = 0.035$) between the expression of these two genes. Interestingly, the negative correlation between *PAX6* and *MMP2* expressions became stronger after excluding astrocytomas from the 91-specimen data set ($R = -0.34$, $P = 0.020$), whereas it lost its significance after excluding GBMs ($R = -0.06$, $P = 0.682$). These data suggest that PAX6-mediated suppression of *MMP2* expression occurs in GBM, but not in astrocytomas.

Discussion

To delineate the function of PAX6 in suppressing the tumorigenecity of GBM cells, we studied the role of PAX6 in suppressing the invasiveness of GBM cells *in vitro*. We showed evidence that stable overexpression of PAX6 dramatically reduces the cell invasiveness of two GBM cell lines, and *MMP2* is a downstream target gene of PAX6. Interestingly, the effect of PAX6 on *MMP2* expression varies between *in vitro* and *in vivo* settings, ~50% reduction *in vitro* but almost abolished *in vivo*.

GBMs are highly invasive and are known to have lower *PAX6* expression compared with adjacent normal tissues and anaplastic astrocytomas (7). In addition to decreased expression of *PAX6*, several reports described increased expression of *MMP2* in GBMs (25–30), which can be associated with the invasive nature of GBM.

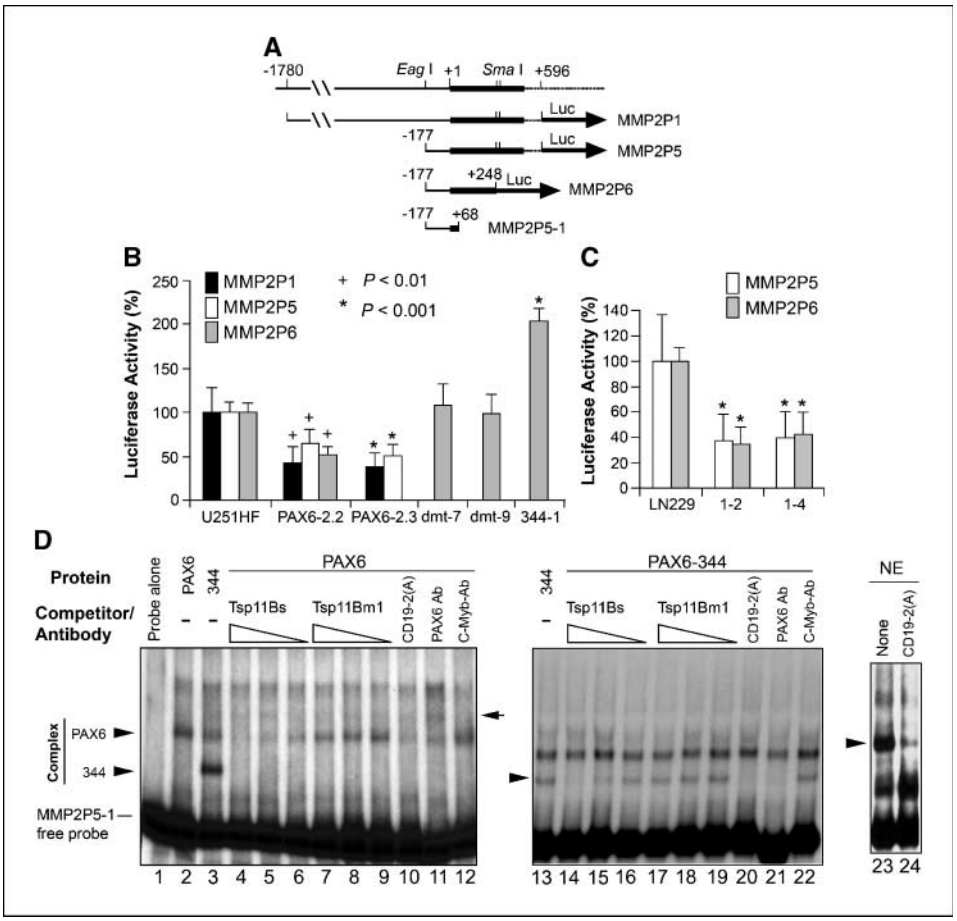

Figure 5. PAX6 binds directly to *MMP2* promoter and suppresses *MMP2* promoter activity in glioma cells. *A,* depiction of the *MMP2* promoter constructs in the luciferase reporter vector pGL3B and probe location using EMSA. MMP2 promoter activity in U251HF and its stable transfectants of PAX6 and PAX6-344 (*B*) and in LN229 and its stable transfectants of PAX6 (*C*) after transient transfection with three *MMP2* promoter luciferase constructs: MMP2P1/pGL3B (*black* column), MMP2P5/pGL3B (*white column*), or MMP2P6/pGL3B (*gray column*). *Columns,* group mean from three to five independent experiments at three repeats per experiment; *bars,* SD. *D,* EMSA narrowed PAX6 binding to a 245-bp region in *MMP2* promoter, MMP2P5-1, using *in vitro* synthesized PAX6 (*lanes 1-12*) or PAX6-344 (*344*; *lanes 12-22*), or nuclear extract from U251HF cells (*lanes 23* and *24*) with the [α-^{32}P]-labeled MMP2P5-1. PAX6 binding specificity was determined by addition of PAX6- or paired domain–binding competitors Tsp11Bs or CD19, respectively, mutant oligomers of Tsp11Bs (Tsp11Bm1), and rabbit antibodies for PAX6 (*PAX6 Ab*) and C-Myb (*C-Myb Ab*). *Minus,* no addition of competitor/antibody; *arrowheads*, MMP2P5-1/PAX6 complex or MMP2P5-1/PAX6-344 complex; *arrow*, supershifted complex of PAX6 antibody/PAX6/MMP2P5-1. Data from each promoter and experiment were converted to percentages of the mean value for its control (U251HF with same promoter), square root transformed to stabilize variance, then analyzed by mixed model ANOVA. Post hoc comparisons were of noncontrols to same-promoter controls. Symbols above noncontrol columns indicate Bonferroni-adjusted *P* values for difference from U251HF.

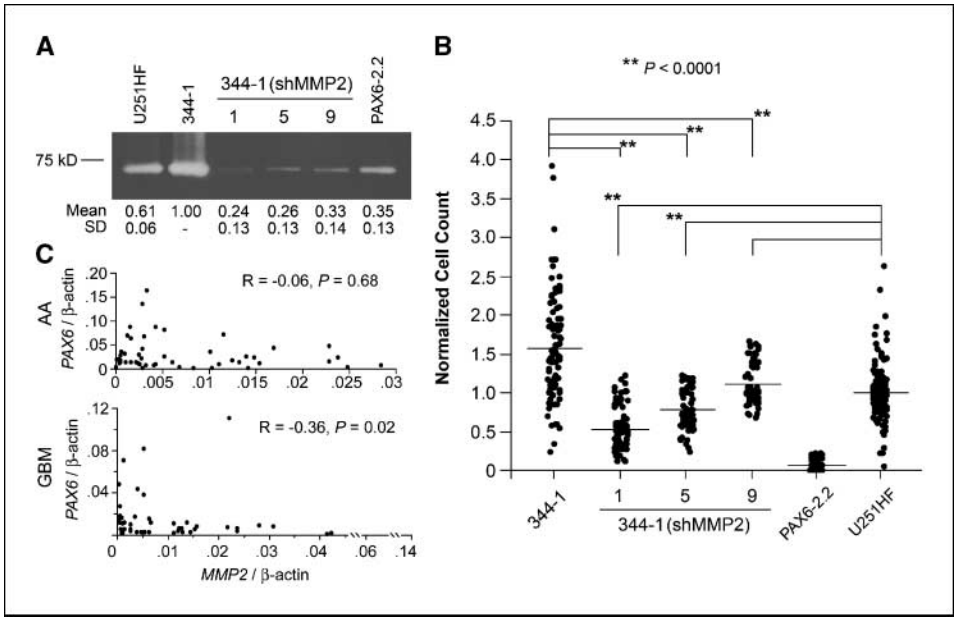

Figure 6. MMP2 is one of the PAX6 target genes mediating PAX6 suppression of glioma cell invasion and reverse correlation between *PAX6* and *MMP2* expression in GBM. *A,* gelatin zymography assay showing knocked down MMP2 protein secreted from a 344 stably transfected U251HF (*344-1*) after stable expression of inhibitor RNA of MMP2 from retroviral construct V2HS-48431, as described in Materials and Methods. *B,* comparison of cell invasiveness by Matrigel invasion assay of three 344-1(shMMP2) clones with different levels of MMP2. Invasion data for the wild-type cells (U251HF) and a PAX6-transfected line (PAX6-2.2) were included for comparison. The invaded cell counts were normalized to U251HF. The position of the bar is the mean of the normalized cell counts from duplicate or triplicate invasion assays of three to five independent experiments. Bonferroni-adjusted $P < 0.0001$ from Wilcoxon rank-sum tests was used for statistically significant difference between groups. *C,* depictions of correlations between the *PAX6* and *MMP2* expression ratios relative to β-actin in 43 astrocytomas and 7 adjacent normal tissues (*top*) and 41 GBMs and 7 adjacent normal tissues (*bottom*). Spearman correlation coefficients (*R* value) and the significance (*P* value) are shown.

The negative correlation between the expression of *PAX6* and *MMP2* in GBMs found in this study supports the conclusions that changing PAX6 functionality can change the invasiveness of and the *MMP2* expression in GBM cell lines. Clearly, *MMP2* is one of the mediators of PAX6 suppression of GBM cell invasion. However, our data also showed that *MMP2* is not the only PAX6-regulated gene that affects invasion. Data from our microarray comparison of gene expressions in PAX6 transfected U251HF cells showed an alteration in the expression of other genes involved in promoting cell invasion. Some of these genes, such as the gene encoding platelet-derived growth factor receptor α, have been confirmed by real-time quantitative RT-PCR (41).

Two regulatory mechanisms for *MMP2* overexpression in gliomas have been postulated from *in vitro* assay data using stably transfected glioma cell lines: (*a*) suppression of *MMP2* expression via PTEN (42); (*b*) activation of *MMP2* expression via insulin-like growth factor binding protein 2 (IGFBP2; ref. 43). Our data suggest a new regulatory mechanism for *MMP2* expression, which is typically found to be up-regulated in GBM, via the transcription factor PAX6. Under *in vitro* culture conditions, *PTEN* gene expression levels were not altered in U251HF PAX6 stable transfectants (data not shown). In addition, in U251HF cells, PAX6-mediated regulation of *MMP2* expression did not seem to be via IGFBP2. *In vitro* cultured U251HF cells expressed very low levels of *IGFBP2*, which did not change after expressing exogenous PAX6 (data not shown). Thus, *MMP2* expression in gliomas seems to be regulated by at least three independent pathways mediated via PTEN, IGFBP2, and PAX6.

Our *MMP2* promoter assay and EMSA data suggest that *MMP2* is a downstream target gene of PAX6 in GBM cells. We have narrowed a PAX6-responsive region in the proximal *MMP2* promoter to a 245-bp sequence (MMP2P5-1). This PAX6 direct binding to the *MMP2* promoter did not require the full-length COOH-terminal PST domain. To our knowledge, this is the first report of PAX6 acting as a *trans*-repressor. PAX6 has been reported as a *trans*-activator (39). In fact, PAX6 has been shown to bind and activate the promoter of another MMP gene encoding the 92-kDa gelatinase B (*MMP9*) in cultured corneal epithelial cells (44). Searches against the MMP2P5-1 sequence for known PAX6 binding sites failed to identify any region with high sequence similarity to reported PAX6 binding sites, including the PAX6 binding site in *MMP9*. This suggests that a novel PAX6 binding site exists within this 245-bp region of the *MMP2* promoter. In contrast to the suppression effect of PAX6 on *MMP2* expression, PAX6-344 enhanced *MMP2* expression and promoter activity, indicating that the PST domain of PAX6 is critical to this repressor function. In addition, this finding supports previous reports that showed a dominant negative function for this truncation mutant in regulating gene expression (39).

Overall data from this study further support the suppressive function of PAX6 in glioma progression and delineate its underlying mechanism: suppression of cell invasiveness by repressing the expression of proinvasive genes such as *MMP2*. Attenuation of *PAX6* expression in GBM may account for the increased cell invasiveness and/or other processes responsible for tumor progression. A therapy that combats this loss may prove to be beneficial in treating this disease.

Acknowledgments

Received 10/26/2005; revised 7/20/2006; accepted 8/16/2006.

Grant support: National Brain Tumor Foundation Pediatric Brain Tumor Grant, Arkansas Cancer Research Center Tobacco Settlement Fund, The University of Arkansas for Medical Science College of Medicine Pilot Fund, American Cancer Society Pilot Study Grant, Fraternal Order of Eagles, and USPHS grant RR020146.

The costs of publication of this article were defrayed in part by the payment of page charges. This article must therefore be hereby marked *advertisement* in accordance with 18 U.S.C. Section 1734 solely to indicate this fact.

References

1. CBTRUS. Statistical report: primary brain tumors in the United States, 1997-2001. Central Brain Tumor Registry of the United States; 2004.
2. Kleihues P, Cavenee WK. Pathology and genetics of tumor of the nervous system. Lyon (France): IARC Press; 2000. p. 9–54.
3. Sposto R, Ertel IJ, Jenkin RD, et al. The effectiveness of chemotherapy for treatment of high grade astrocytoma in children: results of a randomized trial. A report from the Childrens Cancer Study Group. J Neurooncol 1989;7: 165–77.
4. Fine HA, Dear KB, Loeffler JS, et al. Meta-analysis of radiation therapy with and without adjuvant chemotherapy for malignant gliomas in adults. Cancer 1993;71: 2585–97.
5. Stewart LA. Chemotherapy in adult high-grade glioma: a systematic review and meta-analysis of individual patient data from 12 randomised trials. Lancet 2002;359: 1011–8.
6. Zhou YH, Wu X, Tan F, et al. PAX6 suppresses growth of human glioblastoma cells. J Neurooncol 2005;71: 223–9.
7. Zhou YH, Tan F, Hess KR, et al. The expression of PAX6, PTEN, vascular endothelial growth factor, and epidermal growth factor receptor in gliomas: relationship to tumor grade and survival. Clin Cancer Res 2003; 9:3369–75.
8. Callaerts P, Halder G, Gehring WJ. PAX-6 in development and evolution. Annu Rev Neurosci 1997;20: 483–532.
9. Chi N, Epstein JA. Getting your Pax straight: Pax proteins in development and disease. Trends Genet 2002;18:41–7.
10. Stoykova A, Gruss P. Roles of Pax-genes in developing and adult brain as suggested by expression patterns. J Neurosci 1994;14:1395–412.
11. Nacher J, Varea E, Blasco-Ibanez JM, et al. Expression of the transcription factor Pax6 in the adult rat dentate gyrus. J Neurosci Res 2005;81:753–61.
12. Collinson JM, Chanas SA, Hill RE, et al. Corneal development, limbal stem cell function, and corneal epithelial cell migration in the Pax6(+/−) mouse. Invest Ophthalmol Vis Sci 2004;45:1101–8.
13. Nomura T, Osumi N. Misrouting of mitral cell progenitors in the Pax6/small eye rat telencephalon. Development 2004;131:787–96.
14. Chapouton P, Gartner A, Gotz M. The role of Pax6 in restricting cell migration between developing cortex and basal ganglia. Development 1999;126:5569–79.
15. Jimenez D, Lopez-Mascaraque L, de Carlos JA, et al. Further studies on cortical tangential migration in wild type and Pax-6 mutant mice. J Neurocytol 2002;31: 719–28.
16. Engelkamp D, Rashbass P, Seawright A, et al. Role of Pax6 in development of the cerebellar system. Development 1999;126:3585–96.
17. Hamasuna R, Kataoka H, Moriyama T, et al. Regulation of matrix metalloproteinase-2 (MMP-2) by hepatocyte growth factor/scatter factor (HGF/SF) in human glioma cells: HGF/SF enhances MMP-2 expression and activation accompanying up-regulation of membrane type-1 MMP. Int J Cancer 1999;82:274–81.
18. Qin H, Moellinger JD, Wells A, et al. Transcriptional suppression of matrix metalloproteinase-2 gene expression in human astroglioma cells by TNF-α and IFN-γ. J Immunology 1998;161:6664–73.
19. Zhang D, Brodt P. Type 1 insulin-like growth factor regulates MT1-MMP synthesis and tumor invasion via PI 3-kinase/Akt signaling. Oncogene 2003;22:974–82.
20. Giannelli G, Falk-Marzillier J, Schiraldi O, et al. Induction of cell migration by matrix metalloprotease-2 cleavage of laminin-5. Science 1997;277:225–8.
21. McCawley LJ, Matrisian LM. Matrix metalloproteinases: they're not just for matrix anymore! Curr Opin Cell Biol 2001;13:534–40.
22. Dong J, Opresko LK, Dempsey PJ, et al. Metalloprotease-mediated ligand release regulates autocrine signaling through the epidermal growth factor receptor. Proc Natl Acad Sci U S A 1999;96:6235–40.
23. Platten M, Wick W, Weller M. Malignant glioma biology: role for TGF-β in growth, motility, angiogenesis, and immune escape. Microsc Res Tech 2001;52:401–10.
24. Bergers G, Brekken R, McMahon G, et al. Matrix metalloproteinase-9 triggers the angiogenic switch during carcinogenesis. Nat Cell Biol 2000;2:737–44.
25. Nakada M, Nakamura H, Ikeda E, et al. Expression and tissue localization of membrane-type 1, 2, and 3 matrix metalloproteinases in human astrocytic tumors. Am J Pathol 1999;154:417–28.
26. Rooprai HK, Van Meter T, Rucklidge GJ, et al. Comparative analysis of matrix metalloproteinases by immunocytochemistry, immunohistochemistry and zymography in human primary brain tumours. Int J Oncol 1998;13:1153–7.
27. Yamamoto M, Mohanam S, Sawaya R, et al. Differential expression of membrane-type matrix metalloproteinase and its correlation with gelatinase A activation in human malignant brain tumors *in vivo* and *in vitro*. Cancer Res 1996;56:384–92.
28. Raithatha SA, Muzik H, Rewcastle NB, et al. Localization of gelatinase-A and gelatinase-B mRNA and protein in human gliomas. Neuro-oncol 2000;2: 145–50.
29. Levicar N, Nutall RK, Lah TT. Proteases in brain tumour progression. Acta Neurochir (Wien) 2003;145: 825–38.
30. Zhou YH, Hess RK, Liu L, et al. Modeling prognosis for patients with malignant astrocytic gliomas: quantifying the expression of multiple genetic markers and clinical variables. Neuro-oncol 2005;7:485–94.
31. Ishii N, Maier D, Merlo A, et al. Frequent co-alterations of TP53, p16/CDKN2A, p14ARF, PTEN tumor suppressor genes in human glioma cell lines. Brain Pathol 1999;9:469–79.
32. Ke LD, Shi YX, Im SA, et al. The relevance of cell proliferation, vascular endothelial growth factor, and basic fibroblast growth factor production to angiogenesis and tumorigenicity in human glioma cell lines. Clin Cancer Res 2000;6:2562–72.
33. Zheng JB, Zhou YH, Maity T, et al. Activation of the human PAX6 gene through the exon 1 enhancer by transcription factors SEF and Sp1. Nucleic Acids Res 2001;29:4070–8.
34. Tang HK, Chao LY, Saunders GF. Functional analysis of paired box missense mutations in the PAX6 gene. Hum Mol Genet 1997;6:381–6.
35. Nirmala C, Jasti SL, Sawaya R, et al. Effects of radiation on the levels of MMP-2, MMP-9 and TIMP-1 during morphogenic glial-endothelial cell interactions. Int J Cancer 2000;88:766–71.
36. Huhtala P, Chow LT, Tryggvason K. Structure of the human type IV collagenase gene. J Biol Chem 1990;265: 11077–82.
37. Zhou YH, Zheng JB, Gu X, et al. Novel PAX6 binding sites in the human genome and the role of repetitive elements in the evolution of gene regulation. Genome Res 2002;12:1716–22.
38. Prosser J, van Heyningen V. PAX6 mutations reviewed. Hum Mutat 1998;11:93–108.
39. Tang HK, Singh S, Saunders GF. Dissection of the transactivation function of the transcription factor encoded by the eye developmental gene PAX6. J Biol Chem 1998;273:7210–21.
40. Epstein J, Cai J, Glaser T, et al. Identification of a Pax paired domain recognition sequence and evidence for DNA-dependent conformational changes. J Biol Chem 1994;269:8355–61.
41. Zhou Y-H, Glass T, Yung WKA. PAX6 down-regulate the expression of PDGFRA and MCP-1 genes in glioblastoma cells. Neuro-oncol 2001;3:312.
42. Koul D, Parthasarathy R, Shen R, et al. Suppression of matrix metalloproteinase-2 gene expression and invasion in human glioma cells by MMAC/PTEN. Oncogene 2001;20:6669–78.
43. Wang H, Shen W, Huang H, et al. Insulin-like growth factor binding protein 2 enhances glioblastoma invasion by activating invasion-enhancing genes. Cancer Res 2003;63:4315–21.
44. Sivak JM, Mohan R, Rinehart WB, et al. Pax-6 expression and activity are induced in the reepithelializing cornea and control activity of the transcriptional promoter for matrix metalloproteinase gelatinase B. Dev Biol 2000;222:41–54.

PAX6 Suppresses the Invasiveness of Glioblastoma Cells and the Expression of the Matrix Metalloproteinase-2 Gene

Debra A. Mayes, Yuanjie Hu, Yue Teng, et al.

Cancer Res 2006;66:9809-9817.